Journal of Geomatics Vol. 18, No. 2, October 2024

Selection of Optimum Enhancement Technique for the Discrimination of Alkali Granites and Syenites around Suryamalai Batholith of Central Tamil Nadu, India

Muthamilselvan A
Department of Remote Sensing, Bharathidasan University, Trichy, 620 023
Email: thamil1978@gmail.com

(Received on 7 September 2023; in final form 12 September 2024)

***DOI**: https://doi.org/10.58825/jog.2024.18.2.111*

Abstract: Image processing techniques currently have become inseparable in lithological and alteration zone mapping. In the present study, Landsat OLI satellite image has been used to identify alkali syenite and granites of Suryamalai batholith, central Tamil Nadu. For lithological discrimination, various types of image enhancement techniques were applied. The analyses have indicated that only the following techniques like Kaufmann's ratio, band ratio of 5/7, 3/1 and 3/5 and supervised classification were found to be suitable for the decimation of alkali syenite and granites. In addition, it was also noticed that the band ratio of 5/7, 3/1 and 3/5, Crosta technique and thermal reclassification have enabled to discriminate the metamorphic rocks into fissile hornblende biotite gneiss and hornblende biotite gneiss. Further, the image classification techniques were found to be suitable to distinguish phase I and phase III granites in the study area as brought out by the earlier studies based on the grain size variations, colour and mineral content of the rock types.

Keywords: Image processing, Landsat OLI, Alkali syenite, granite Suryamalai batholith

1. Introduction

Recognizing the spatial patterns of geological mapping is crucial for geoinformatics to be one of the standard and most successful procedures in the field of exploration geology. This tool is extremely powerful and essential for geologists to enhance the regional geological mapping process (Pour &Hashim, 2015). The use of satellite data has the potential to solve the challenges and limitations associated with geological exploration. Recent advancements in multi-spectral remote sensing systems, such as the advanced spaceborne thermal emission and reflection radiometer (ASTER), have demonstrated the usage of satellite imagery for geological mapping with various purposes around the world (Di Tommaso & Rubinstein, 2007; Liu et. al, 2014; Masoumi et. al., 2017; Pour et.al., 2017; Van Ruitenbeek et. al., 2012).

The use of band ratio and principal component analysis is widespread in mapping mineral alteration and lithological discrimination (Ahmed Madani, 2014, A. Muthamilselvan 2016). In 2016, Norbert Simon utilized 25 different ways to enhance the band ratio image on the Landsat 5TM image for discrimination of different lithologies. Furthermore, it was discovered that these combinations enhance the textural information of different rock type, which can be indirectly utilised for discrimination diverse lithologies. A. Muthamilselvan (2016) has employed supervised classification and the Crosta technique in the process of detecting lithological differences using digital image processing techniques in an ENVI environment. By employing Landsat ETM+ digital imagery, he was able to identify the litho-contacts between alwar and ajabgarh quartzite in the south-western region of the North Delhi Fold Belt (NDFB) on the basis of the argillaceous and arenaceous nature of the rocks.

According to Sabin (1999), the best outcomes can be achieved by combining geologic and fracture mapping with the recognition of hydrothermally altered rocks. The spectral bands of Landsat TM, ETM+, and OLI are well suited for recognizing accumulations of alteration zones related to hydrothermal activity. Since the 1970s, scientists have created various image processing techniques, including band ratio, principal component analysis (PCA), supervised and unsupervised classification, to discriminate mineral alteration zones effectively. In this present study, Landsat 8 OLI satellite imagery has been applied to discriminate between rock types. Spectral information has been used to discriminate alkali syenites from alkali granite and also to demarcate the lithocontacts between igneous and metamorphic rocks.

Landsat bands are utilized for distinct purposes, including band 7 for geology, band 5 for distinguishing between soil and rock, and band 3 for discrimination of soil from vegetation. (Boettinger et al., 2008; Campbell, 2002; Chen and Campagna, 2009).

2. Geological setting

The study area is located in the southern part of the Indian peninsula and is made up of various metals and minerals, such as barite, chromite, iron, magnesite, pyrite, beryl, ruby, pyrochlore, columbite-tantalite, etc. Major rock types include hornblende biotite gneiss, fissile hornblende biotite gneiss, calc granulite, carbonatite, syenites, and granite (Figure 1 & Table 1). Suryamalai batholith (SMB) granitoids in the southern part of the study area show three different phases of granite. SMB characterisations were studied by many geologists and suggested the classification based on field relationships,

grain size, colour variations and the presence of radioactive minerals (Roy and Dhanaraju, 1999).

Table 1. Startigraphical succession of the region

Era	Group	Litho Units
Late to Early Proterozoic	Younger Intrusive	Granite
		Pegmatite
Late Proterozoic	Alkali Complex	Carbonatite
		Syenite
		Dunite
		Epidote Hornblende Gneiss
Archaean	Charnockite Group	Banded Magnetite Quartzite
		Charnockite
	Khondalite Group	Calc-Granulite and Limestone
	Bavani Gneisses	Fissile Hornblende Biotite Gneiss

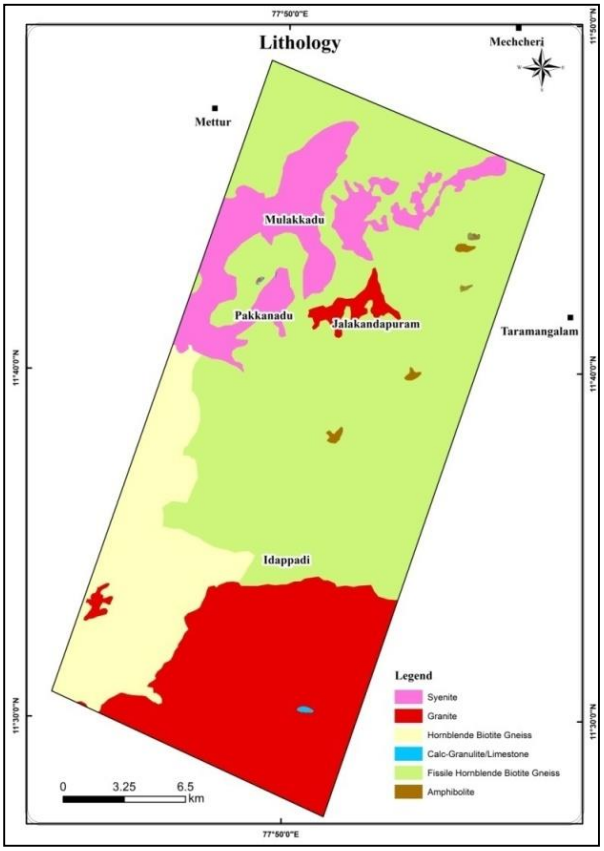

Figure 1. Lithology map of the study area

Phase I granite is made up of medium-grained leucocratic rock that does not have any non-radioactive minerals, In Phase II, gray-colored rocks with a coarse to very coarse grain are observed that contain garnet, opaque, and radioactive minerals; and Phase III granite is very coarse-grained, pink coloured, non-to-weakly radioactive with predominant blocky k-feldspar, pockets of quartz, books of biotite, big octahedral crystals of magnetite, and dodecahedra1 crystals of garnet. Among these, phase I granite was noticed in the periphery of the SMB variants, which occupies a major part of the area and has intruded into the country rock gneiss. Phase II comes next in abundance, and its variable radioactivity and high concentration of garnet, magnetite, and other ore minerals make it easily distinguishable. Phase III is characterized by its pegmatitic nature and limited area extension. The field relationships between these granites demonstrate that phase III has been incorporated into phases I and II, and phase II is intrusive into phase I, all with sharp boundaries, indicating that they are sequentially emplaced into one another.

The spectral signatures of the rock types vary from place to place and are reflected significantly in the satellite imagery. For example, the younger Suryamalai batholiths (SMB) and Sankaridurg dome in the study area exhibit a white tone, whereas the banded magnetite quartzite shows typical linear and curvilinear ridges with contrasting tonal variations (Ramasamy, 1995). Hence, geomatics technology can be effectively used to map the different lithologies that act as stores for metals and minerals in the study area.

3. Methodology and Material used:

The main objective of the study is to select an optimum digital image processing technique to discriminate alkali syenites from alkali granites and to demarcate the contacts of Proterozoic intrusive with Archaean metamorphic rocks. Different image processing techniques, like band ratios, Crosta, supervised classification, and reclassification methods were applied to achieve the best solution. Image processing was performed using Landsat 8 OLI satellite imagery under the ENVI software. Band ratio and PCA analysis were carried out based on the existing methodologies such as Sabin, Crosta, ChicaOlma, Kaufmanns, Crosta analyses etc. Spectral signatures from the existing lithological map of the study area were collected for supervised classification.

Significant variations in litho units and their contacts are i ndicated by the results obtained from the above analyses. Lastly, the accuracy of the outcomes of the methods mentioned earlier was spatially correlated and ground-validated. (Figure 2)

4. Result and Discussion

4.1 Band Ratio Analyses

Remote sensing uses band ratio as a technique for effectively displaying spectral variations for many years. The process of creating a ratio involves dividing the brightness values of one band by another pixel by pixel. Enhancing the contrast between materials is achieved through the division of brightness values at peaks and troughs on a spectral reflectance. This is characterized by enhancing spectral differences and suppressing illumination differences.

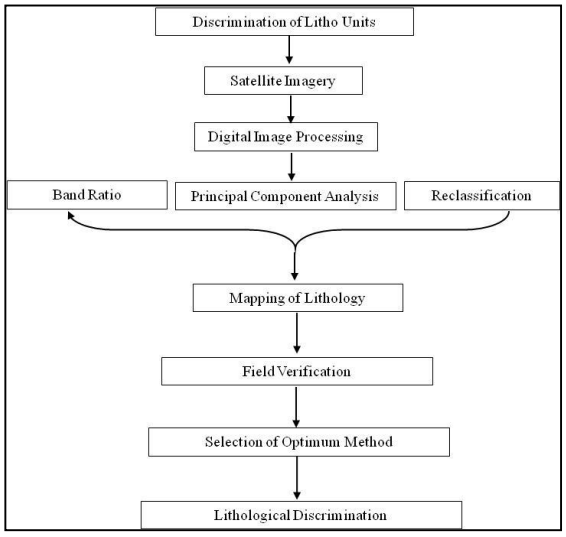

Figure 2. Flow chart of methodology

Differentiating materials can be done using ratios if they have different characteristic spectra (Alexandru et.al., 2007). The enhancement of rock alteration is achieved using the band ratios of Landsat OLI data and it can cause subtle differences in spectral response to be exaggerated. Numerous researchers have developed various band ratios over the years that take advantage of specific reflectance properties of the surface materials. For example, vegetation has an extremely high reflectance in the near infrared wavelength region relative to red wavelengths. The number of possible ratio combinations for a multispectral sensor with K bands is n=K (K-1).

The ratio function can be mathematically expressed as:

$$BVi,j,r = BVi,j,k / BVi,j,l$$

Where,

BVi,j,r = output ratio value of the pixel at i^{th} row and j^{th} column

BVi,j,k = brightness value at the same location for band K.

BVi,j,l = brightness value at the same location for band l

4.1.1 Abram's Ratio:

Abram's ratio was introduced by Abram in 1983. He has used the band ratios 5/7, 3/2 and 4/3 of Landsat ETM data for the red, green and blue (RGB) channels, which are equivalent to 6/7, 4/3 and 5/4 of Landsat 8 and correspond to wavelength regions 1.65 / 2.2 µm, 0.66 / 0.56 µm and 0.83 / 1.65 µm. The results of the band combinations show syenite and granite regions in greenish blue, which indicates the ferric iron charge in the ultraviolet region. Fissile hornblende biotite gneiss shows reddish orange colour, which represents the presence of hydrous minerals absorbed near 2.2µm. The presence of both clay and iron oxide minerals can be seen in the yellow and orange color areas in the composite image. (Abrams, et al., 1983). The yellowish-orange colour from the Abrams ratio has been considered lithocontact between igneous and metamorphic rocks (Figure 3).

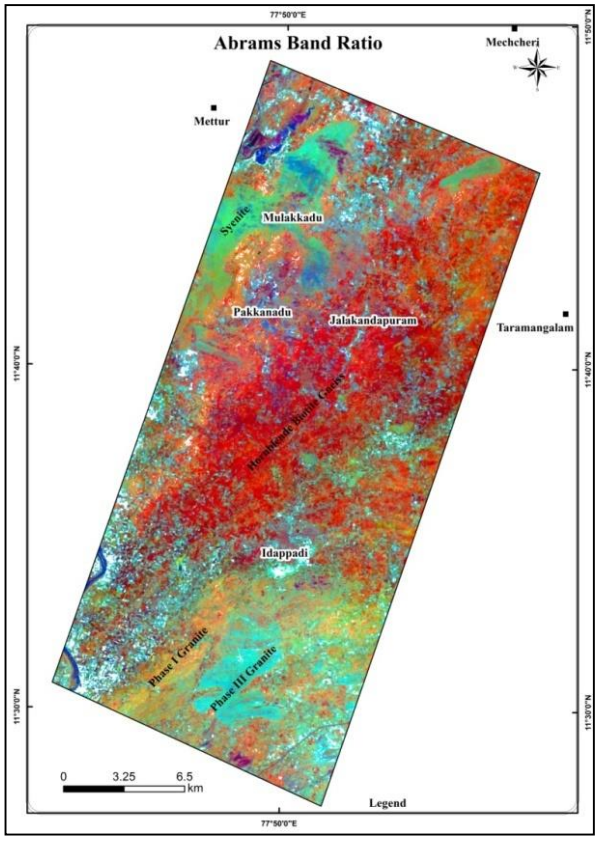

Figure 3. Abram's Ratio

Lithological contacts between igneous and metamorphic rocks were clearly demarcated in the southern (near Idappadi) and northern parts of the study area (Pakkanadu and Mulakkadu) (Figure 3). Further, Phase I (yellowish orange) and Phase III (greenish blue) granites were discriminated perfectly by this ratio. Spectral variation of these rock types is found mainly due to variations in their colour, minerals and grain size in the southern part of the study area (Roy and Dhanaraju, 1999). Phase II granite is similar to Phase I excluding its radioactive nature, which is not prominently differentiated from this ratio analysis.

4.1.2 Kaufmann Ratio:

This ratio was proposed by Kaufmann in 1988. He used Landsat ETM bands 7, 4, 3 and 5 which are equivalent to bands 7, 5, 4 and 6 of Landsat 8 OLI performed in this study. The ratios 7/4, 4/3 and 5/7 ETM thus correspond to the ratios 7/5, 5/4 and 6/7 in OLI data.

According to the result, the band ratio of 5/4 shows vegetation in bright tones because the mesostructure in the NIR band in contrast to the steep fall-off of reflectance towards the visible due to intense chlorophyll absorption (Kaufmann, 1988). The enhancement of clay minerals containing water, micas, carbonates, and hydrates occurs with a band ratio of 6/7. The best enhancement of ferric and ferrous iron occurs with a band ratio of 7/5 because of the major electronic transition bands in the NIR. (at ~ 0.87um). The composite image of 7/5, 5/4, and 6/7 ratios was displayed in RGB colour for further interpretation. The performed image indicates a green and greenish-red colour for phase III granite and syenite rocks respectively. Pinkish violet represents metamorphic rocks

and blue represents granites of phase I origin (Figure 4). This ratio also brought to light a significant difference between phase I and phase III granite in the southern part of the study area. Similarly, litho contacts between granite / syenite and fissile hornblende biotite gneiss were clearly demarcated in the southern as well as in the northern part of the study area.

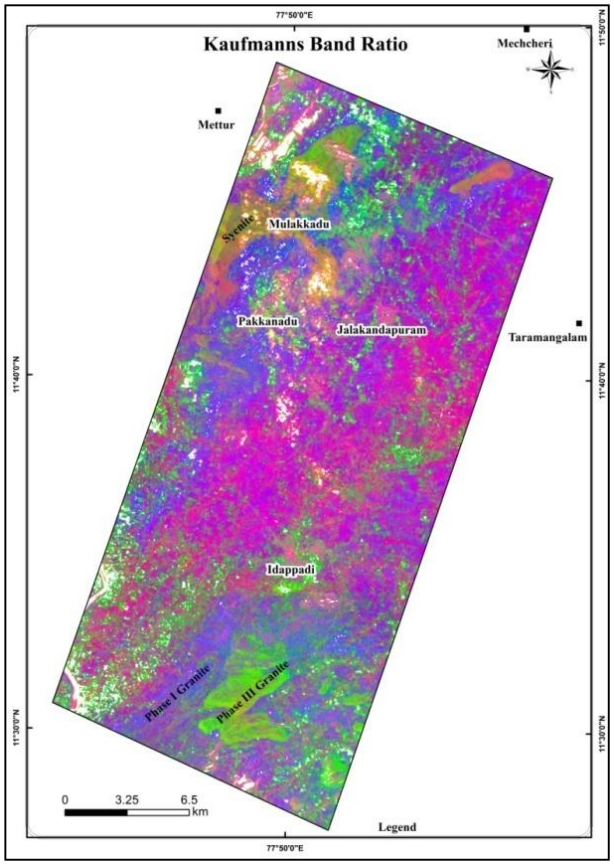

Figure 4. Kaufmann's Ratio

4.1.3 Sabin's Ratio

Sabin (1999) introduced the ratio of 5/7 in red, 3/1 in green and 3/5 in blue for colour composite images, which are taken from Landsat ETM. However, Landsat 8 OLI data has been used for the present study, where the band numbers are varied due to the addition of new coastal aerosol studies. The band ratios for OLI data are 6/7, 4/2, and 4/6, where ratios of 6/7 indicate hydroxyl-bearing minerals and 4/2 indicate iron oxide alteration minerals.

The image (Figure 5) shows yellow as hydrothermal alteration zones, black as water and dark green as vegetation; light green as clay-rich rocks; blue shows sand; red, pink or magenta indicate minerals rich in iron oxides (Sabin, 1999).

The composite image indicates pale blue and dark blue colour for phase I and III granite respectively. Phase III granite and syenite rock almost express the same colour, which is very difficult to discriminate by this ratio (Figure 5). Litho contacts between SMB granitoids and fissile hornblende biotite gneiss were poorly demarcated in the southern part of the study area.

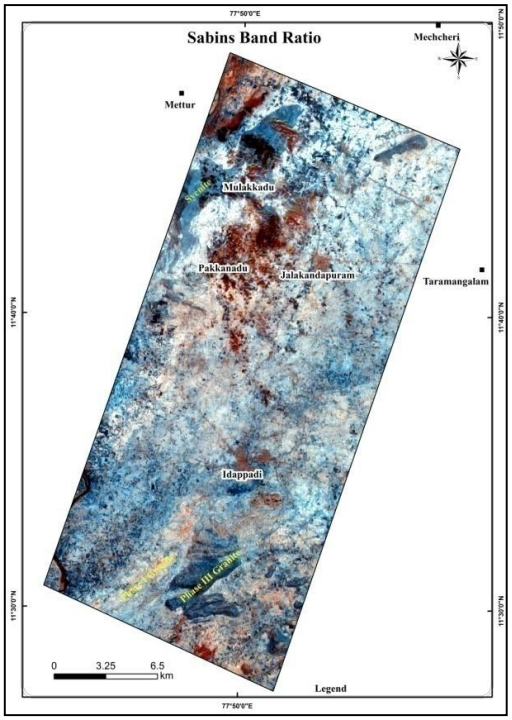

Figure 5. Sabin's ratio

4.1.4 Chica-Olma's Ratio

This ratio was introduced by Chica-Olma (Kudamnya et. al., 2014), in which, bands 7, 5, 4, 3, and 1 have been used for rationing. The Chica-Olma ratios 5/7, 5/4, and 3/1 are responsible for enhancing the color of hydrothermally altered clay minerals in red, ferrous iron as green, and ferric iron as blue, respectively, as shown in Figure 6. When compared to the other band ratio techniques, ChicaOlma's ratio perfectly discriminated the boundary of younger intrusives.

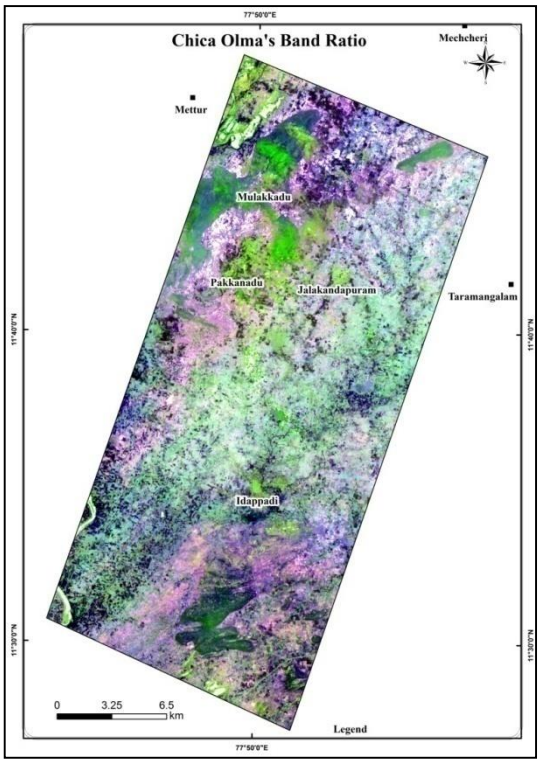

Figure 6. Chica-Olma Ratio

The resulting image indicates the contact of dark green and purple colour in the southern part of the image as phase III and phase I granite rocks respectively. Contacts of purple and light green colour near Idappadi and its southwestern part represent Phase I granite and metamorphic rocks (Figure 6). This ratio also brought to light a significant difference between phase III granite (greenish black) in the southern part of the study area and syenite (bright green) located in the northern part of the image. Further, litho contacts between SMB granitoids and fissile hornblende biotite gneiss were clearly demarcated in the southern as well as in the northern part of the study area.

4.1.5 Band Combinations: 4/2, 6/7 and 10:

In this approach, ratios 4/2 and 6/7 have been taken up along with TIRS band 10 and colour composite images were produced for better visual interpretation. Alkali syenite (dark brown) and phase III granite (greenish brown colour) were discriminated from this approach. Litho contacts between phase I (light green) and phase III granites were clearly seen in the southern part of the study area. In addition, the band ratio also brought to light a significant difference between hornblende biotite gneiss and fissile hornblende biotite gneiss around the Idappadi region. This ratio provided much better information about the rock types compared to the previous methods like Sabin, ChicaOlma, Kaufmanns etc. (Figure 7).

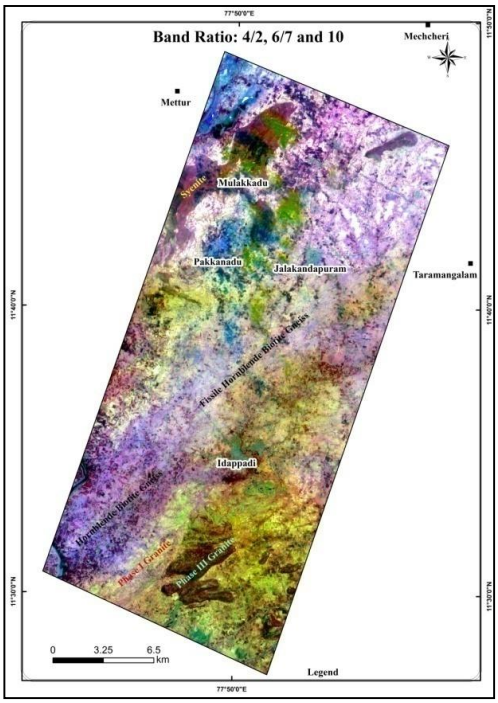

Figure 7. Band Ratio 4/2, 6/7 and 10

4.1.6 Band Combinations: 5/7, 3/1 and 3/5:

Ratios 5/7, 3/1 and 3/5 have also been taken up for the discrimination of rock types. The colour composite image shows a significant difference between alkali syenite (dark brown) and alkali granite (reddish orange). Litho contacts between phase I and phase III granites, granite/syenite, and metamorphic rocks were prominently demarcated from this approach. Further, the difference between hornblende biotite gneiss (dark blue) and fissile hornblende biotite gneiss (light blue) was clearly seen in the composite image. This ration is one of the best and optimum methods for discriminating alkali syenite from alkali granite in phase III and also for the contact of SMB granitoids with metamorphics. (Figure 8).

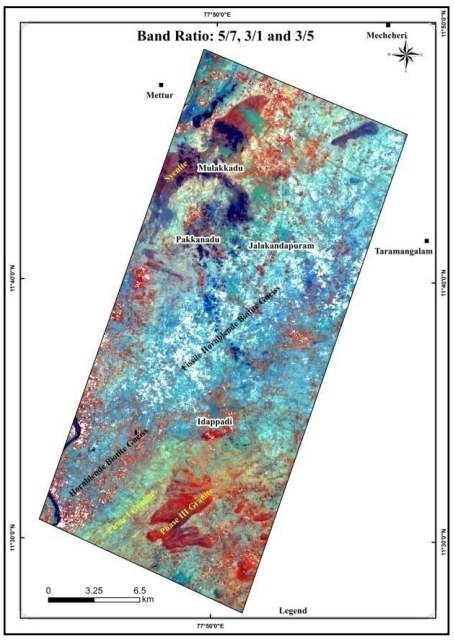

Figure 8. Band Ratio 5/7, 3/1 and 3/5

4.1.7 Band Combinations: 6/7, 4/2 and 5/4

Another band ratio of 6/7, 4/2 and 5/4 has also tried to differentiate various rock types present in the study area. In this approach, alkali syenite and alkali granite were not discriminated against, and both rocks were shown a deep blue colour in the composite image. It was also found that there is a lack of sharp contact between SMB granitoids and fissile hornblende biotite gneiss. However, the performed analysis shows a better contrast between phase I and III granite (Figure 9).

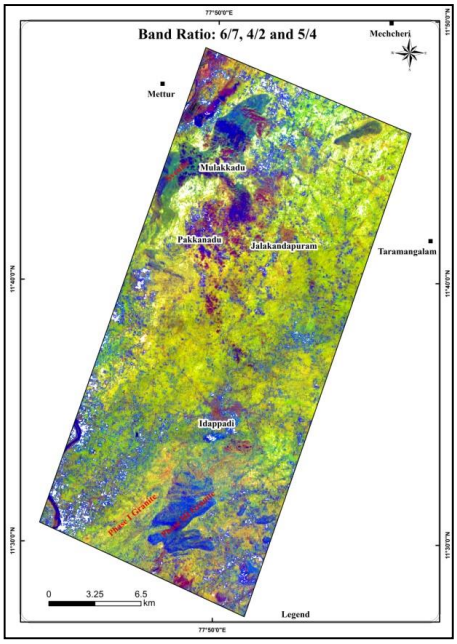

Figure 9. Band Ratio 6/7, 4/2 and 5/4

4.2 Crosta Analysis

The Crosta technique is commonly utilized to locate alteration zones for mineral exploration. This technique was used to distinguish various rock types in the study area. Landsat OLI bands 2, 4, 6 and 7 have been transformed into principal component analysis (PCA) from which PCA 4, 5 and the average of 4 & 5 (Figure 10) have been derived and stacked to get a composite image. The selected bands are believed to be above the intended target and this is known from the Crosta image. Theoretically, the iron oxide minerals and hydroxyl-bearing minerals have absorption bands in the range of bands 2 and 7. in the OLI data. PCA4 enhances hydroxyl minerals for alteration zones by a bright colour. PCA5 enhances the iron oxide mineral for alteration zones, showing a bright colour.

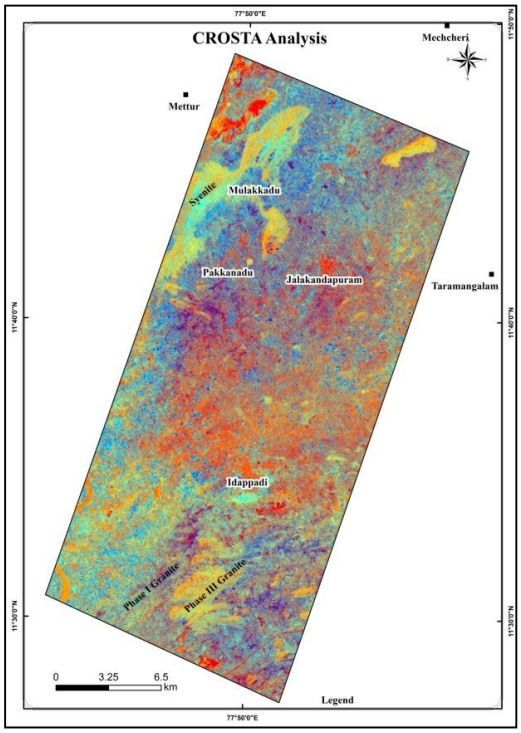

Figure 10. Crosta Analysis (PCA)

The colour composite image obtained from Crosta analysis indicates a minor difference between alkali syenite and alkali granite. Litho contacts between phase I and phase III granites and syenite/granite with metamorphic rocks were significantly delineated by this approach. The difference between hornblende biotite gneiss and fissile hornblende biotite gneiss is also clearly distinguished from this method.

Further, it is found that Crosta analysis is also one of the best and optimum methods, like band ratios of 5/7, 3/1 and 3/5 for the discrimination of various metamorphic rocks.

4.3 PAN Reclassification

PAN data has been reclassified to distinguish the various rock types present in the study area. Panchromatic data has a 15-meter spatial resolution, which was reclassified into 4 categories based on the pixel values (DN values). Spectral signatures played a major role in the discrimination between different rock types. Performed analysis flawlessly discriminated SMB granitoids from fissile hornblende biotite gneiss. However, phase III granite and syenite have been poorly classified. The core of the SMB granitoids is occupied by phase III granite and the periphery by phase I granite, which is significantly discriminated against by this reclassification process. The contact of sharp sky blue with reddish orange in the colour composite image indicates phase I and fissile hornblende biotite gneiss respectively (Figure 11).

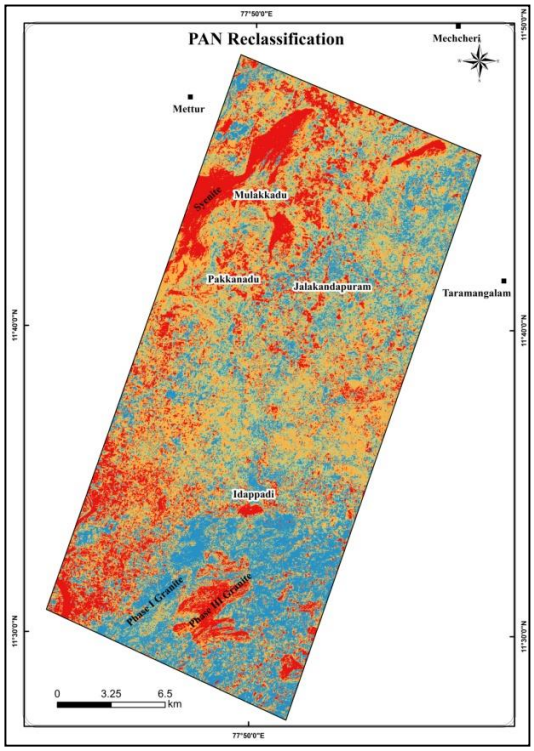

Figure 11. PAN Reclassification

4.4 Thermal Reclassification

Thermal remote sensing is a method that measures the radiation emitting from the ground of an entity. Thermal data from Landsat satellite imagery with a spatial resolution of 100 meters (band 10) has been taken up for lithological discrimination. The thermal band has been reclassified into four types based on the thermal radiant temperature of various rock types. This analysis perfectly discriminated between intrusive rocks such as alkali syenite, granite and hornblende biotite gneiss rocks. However, granite and syenite have once again been poorly classified by method. Granite phase I (orange colour) and III (deep blue) in the colour composite image show a significant difference in the southern part of the study area (Figure 12).

4.5 Supervised Classification

To select training sets (spectral signatures). in supervised classification, the analyst utilized their prior knowledge acquired from the field survey, district resource map, and other secondary data. The computer grouping and assigning each pixel with similar characteristics to their respective class was done using the signature file defined by the analyst. The spectral signatures for granite have been collected from phase III granite to differentiate the

alkali syenite from granite. The classified image significantly brought to light the difference between phase III granite and alkali syenite. However, the litho-contact between phase I granite and metamorphic rocks was poorly classified. These differences have been noticed mainly due to the collection of signatures filed by the analyst (Figure 13).

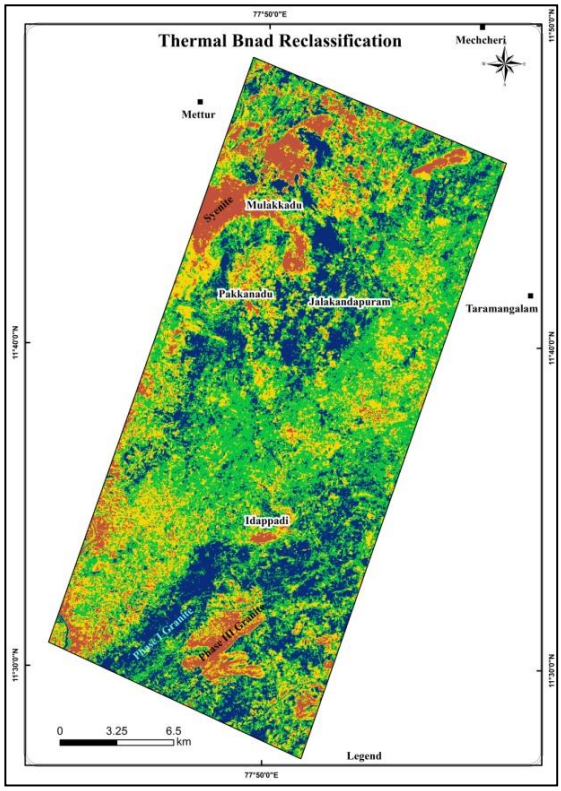

Figure 12. Thermal Reclassification

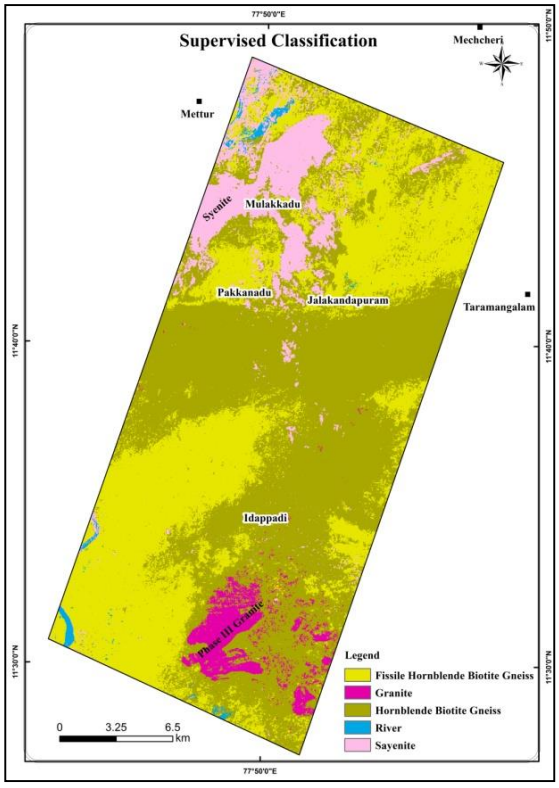

Figure 13. Supervised Classification

4.6 Unsupervised Classification

Unsupervised classification involves pixel-based classification where the user specifies the number of classes. The creation of spectral classes is solely based on numerical information, which is pixel values for each band. The pixels are grouped together based on their spectral similarity. In this approach, six classes were assigned by the analyst to differentiate the various rock types that occurred in the study area. Unsupervised classification significantly brought out the contact between SMB granitoids and metamorphic rocks, particularly fissile hornblende biotite gneiss. Alkali syenite and granite of phase III were weakly demarcated from this approach. However, the performed analysis discriminated perfectly between phase I granite and phase III (Figure 14).

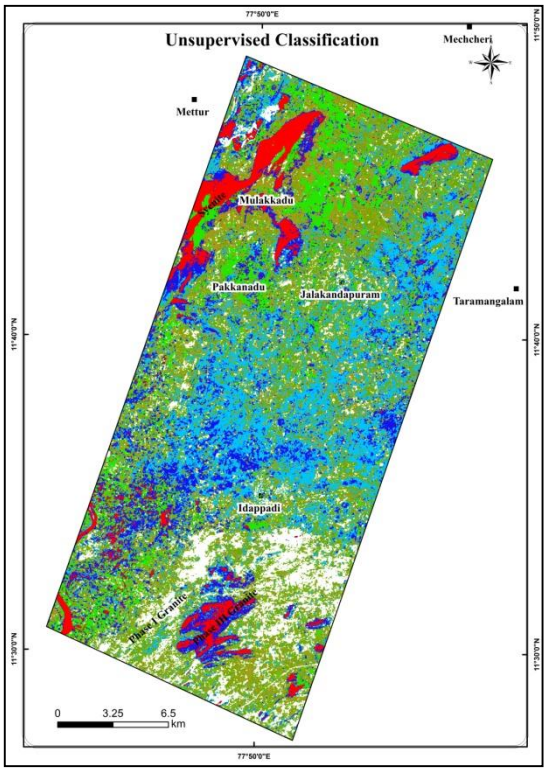

Figure 14. Unsupervised Classification

5. Conclusions

The present study demonstrates the effectiveness of image enhancement techniques like band ratio, PCA, supervised, unsupervised classification, Pan and thermal reclassification to discriminate lithological units present in the study area. 12 types of image enhancement techniques have been performed, in which Kaufmann's band ratios of 7/5, 5/4 and 6/7 and ratios of 5/7, 3/1 and 3/5 clearly discriminated against various rock types in the study area. Each of Landsat's band can be used for specific purposes, including band 7 for geology, band 5 for distinguishing soil from rock, and band 3 for discrimination of soil from vegetation. Combinations of these bands produced the best result when compared to the other methods. There was a significant difference between alkali syenite and granite obtained from the supervised classification technique, which was poorly classified from the unsupervised and reclassification techniques. Among the image

enhancement techniques, except supervised classification, all other methods distinguish phase I and phase III granites effectively. Band ratios of 5/7, 3/1 and 3/5, Crosta and thermal reclassification techniques brought to light a significant difference between fissile hornblende biotite gneiss and hornblende biotite gneiss. Based on the study, it can be concluded that Kauffman, supervised classification, and 5/7, 3/1 & 3/5 are the optimum techniques for the discrimination of alkali syenite and granite in the study area.

Acknowledgements: The expressed heartfelt gratitude to the Department of Remote Sensing, Bharathidasan University, for the provision of the GIS Lab and constant encouragement towards research activities.

References

Aalexandru I., M. Cornelia and G. Dorian (2007). Proceedings of the Ninth International Symposium on Symbolic and Numeric Algorithms for Scientific Computing, SYNASC 2007, Timisoara, Romania, 26-29.

Abrams M. J., D. Brown, L. Lepley and R. Sadowski (1983). Remote sensing for porphyry copper deposits in southern Arizona Economic Geology. 78(4), 591-604

Ahmed M. (2014). Assessment and Evaluation of Band Ratios, Brovey and HSV Techniques for Lithological discrimination and Mapping Using Landsat ETM and SPOT-5 Data. International Journal of Geosciences, 5, 5-11

Boettinger J. L., R. D. Ramsey, J. M. Bodily, N.J. Cole, S. Kienast-Brown, S. J. Nield, A. M. Saunders and A. K. Stum (2008). Landsat Spectral Data for Digital Soil Mapping. In Digital Soil Mapping with Limited Data, A.E. Hartemink, A. McBratney, and M. de L. Mendonça Santos, eds. (Dordrecht: Springer Netherlands), 193– 202.

Campbell J. B. (2002) Introduction to remote sensing. The Guilford Press, New York

Chen X. and D. Campagna (2009) Remote Sensing of Geology. In: Warner, T.A., Nellis, M.D. and Foody, G.M., Eds., The SAGE Handbook of Remote Sensing, SAGE, London, 328.

Di Tommaso I. and N. Rubinstein (2007). Hydrothermal alteration mapping using ASTER data in the infiernillo porphyry deposit, Argentina. Ore Geology Reviews, 32,275–290.

Kaufmann H. (1988). Concepts, processing and results. International Journal of Remote Sensing. (10-11), 1639-1658.

Kudamnya E. A, W. T. Andongma and J. Osumeje (2014). Hydrothermal mapping of Maru schist belt, north-western Nigeria using remote sensing technique. International Journal of Civil, 3, 59-66.

Liu L., J. Zhou, D. Jiang, D. Zhuang and I. Mansaray (2014). Lithological discrimination of the mafic-ultramafic complex, Huitongshan, Beishan, China: Using ASTER data. Journal of Earth Science, 25, 529–536.

Masoumi F., T. Eslamkish, A. A. Abkar, M. Honarmand and J. Harris (2017). Integration of spectral, thermal, and textural features of ASTER data using random forests classification for lithological mapping. Journal of African Earth Science, 129, 445–457.

Muthamilselvan A. (2016). Application of Supervised classification and Crosta Technique for Lithological Discrimination in Parts of South Khetri Belt, Sikar District, Rajasthan. Journal of the Indian Society of Remote Sensing, 75, 765, 1-13.

Pour A. B., M. Hashim, J.K. Hong and Y. Park (2017). Lithological and alteration mineral mapping in poorly exposed Lithology using landsat-8 and ASTER satellite data: North-eastern Graham Land, Antarctic Peninsula. Journal of Ore Geology Reviews.108, 112-133.

Pour A. B. and M. Hashim (2015). Structural mapping using PALSAR data in the central gold belt peninsular Malaysia. Ore Geology Reviews, 64, 13–22.

Ramasamy S. M. (1995). Remote Sensing in the inventory of metallogenic environs. Trends in Geological Remote Sensing, Rawat Publication, 97-109.

Roy M., and R. Dhana Raju. (1999). Petrogenetic model of A-type granitoids of the Kullampatti area, Salem district, Tamil Nadu, India. Gond. Res., 2(1): 127-135.

Sabin F. F. (1999). Remote Sensing for Mineral Exploration. Ore Geology Reviews 14:157-183.

Van Ruitenbeek, F. J. A., T. J. Cudahy, F. D. Van der Meer and M. Hale (2012). Characterization of the hydrothermal systems associated with archaeon VMS mineralization at Panorama, Western Australia, using hyper spectral, geochemical and geothermometric data. Ore Geology Reviews, 45, 33–46.